ADVANCES IN ATMOSPHERIC SCIENCES, VOL. 29, NO. 4, 2012, 867–886

Impacts of Multi-Scale Solar Activity on Climate. Part I: Atmospheric Circulation Patterns and Climate Extremes

Hengyi WENG*

State Key Laboratory of Numerical Modeling for Atmospheric Sciences and Geophysical Fluid Dynamics,

Institute of Atmospheric Physics, Chinese Academy of Sciences, Beijing 100029

(Received 18 November 2011; revised 31 January 2012)

ABSTRACT

The impacts of solar activity on climate are explored in this two-part study. Based on the principles of atmospheric dynamics, Part I propose an amplifying mechanism of solar impacts on winter climate extremes through changing the atmospheric circulation patterns. This mechanism is supported by data analysis of the sunspot number up to the predicted Solar Cycle 24, the historical surface temperature data, and atmospheric variables of NCEP/NCAR Reanalysis up to the February 2011 for the Northern Hemisphere winters. For low solar activity, the thermal contrast between the low- and high-latitudes is enhanced, so as the mid-latitude baroclinic ultra-long wave activity. The land-ocean thermal contrast is also enhanced, which amplifies the topographic waves. The enhanced mid-latitude waves in turn enhance the meridional heat transport from the low to high latitudes, making the atmospheric "heat engine" more efficient than normal. The jets shift southward and the polar vortex is weakened. The Northern Annular Mode (NAM) index tends to be negative. The mid-latitude surface exhibits large-scale convergence and updrafts, which favor extreme weather/climate events to occur. The thermally driven Siberian high is enhanced, which enhances the East Asian winter monsoon (EAWM). For high solar activity, the mid-latitude circulation patterns are less wavy with less meridional transport. The NAM tends to be positive, and the Siberian high and the EAWM tend to be weaker than normal. Thus the extreme weather/climate events for high solar activity occur in different regions with different severity from those for low solar activity. The solar influence on the mid- to high-latitude surface temperature and circulations can stand out after removing the influence from the El Niño-Southern Oscillation. The atmospheric amplifying mechanism indicates that the solar impacts on climate should not be simply estimated by the magnitude of the change in the solar radiation over solar cycles when it is compared with other external radiative forcings that do not influence the climate in the same way as the sun does.

Key words: solar impacts on climate, surface thermal contrasts, dynamical amplifying mechanism, atmospheric circulations, climate extremes

Citation: Weng, H.-Y., 2012: Impacts of multi-scale solar activity on climate. Part I: Atmospheric circulation patterns and climate extremes. *Adv. Atmos. Sci.*, **29**(4), 867–886, doi: 10.1007/s00376-012-1238-1.

1. Introduction

In the boreal winters of 2009/2010 and 2010/2011, some severe weather/climate extremes had broken records on interdecadal-centennial timescales. These extremes have attracted much of attention from scientists to ordinary people because of their enormous societal and economical impacts. These two winters are a couple of years after the anomalously low solar minimum between Solar Cycle 23 and Solar Cycle 24, and the predicted Solar Cycle 24 is weaker than previous solar cycles[a]. The consensus about the cause of increased extreme weather/climate in recent decades given by the IPCC (2007) is the global warming, which is considered mainly due to increased human activity. However, some studies on regional climate change, such as over China, have shown discrepancy with the IPCC's consensus (e.g., Zhou and Yu, 2006; Soon et al., 2011). Since the "natural variability" in the two winters seemed to have surpassed the anthropogenic

*Corresponding author: Hengyi WENG, weng@lasg.iap.ac.cn, hengyi_weng@yahoo.com

[a]http://www.swpc.noaa.gov/SolarCycle/SC24/index.html

warming effect, whether solar activity might have impacted on the record-breaking weather/climate events has become an interesting issue for us to explore.

The energy from the sun is the ultimate source to drive atmospheric circulations on the earth, which is closely related to weather and climate events. The atmosphere as a "heat engine" transports the heat from the tropics to the poles through mid-latitude baroclinic waves (e.g., Barry et al., 2002). Such a "heat engine" is more efficient in winter than in summer, since the meridional temperature gradient (baroclinicity) and, therefore, the long waves is more active in winter than in other seasons. To study the solar impacts on climate, it is essential to understand how a small change ($\sim 0.1\%$) in the observed total solar irradiance (TSI) over an 11-yr solar cycle (Lean, 1991) can change the atmospheric circulation patterns and wave activity or the efficiency of the atmospheric "heat engine". If these changes in the atmosphere are large enough to change the location and severity of extreme weather/climate events, then the atmospheric dynamics would play a fundamental amplifying mechanism in the sun-climate relationship.

In the recent decades, more and more evidences of solar influence on climate are presented by both observational and climate modeling studies (e.g., Reid, 1991; Salby and Callaghan, 2004; Kodera and Kuroda, 2005; Weng, 2005; Haigh, 2007; van Loon et al., 2007; Tung and Camp, 2008; Lean and Rind, 2009; Soon, 2009; Soon et al., 2011). In a recent review paper, Gray et al. (2010) summarized two categories of possible mechanism for the climate to respond the variation in solar irradiation: the "top-down" and "bottom-up" mechanisms.

The "top-down" mechanism emphasizes the impacts of the sun's ultraviolet (UV) irradiance on the middle atmosphere first, because the magnitude of change in UV is several times larger than the TSI over an 11-yr solar cycle. The solar influence is then transferred downward through dynamical links between stratosphere and troposphere, and finally reaches the earth surface and changes the surface temperature (e.g., Salby and Callaghan, 2004; Kodera and Kuroda, 2005; Haigh, 2007; Gray et al., 2010; Ineson et al., 2011). The "bottom-up" mechanism is through the direct TSI effects at the surface involving solar energy absorption. van Loon et al. (2007) and Meehl et al. (2008) presented that the 11-yr solar cycle at its peaks strengthens the climatological precipitation maxima in the tropical Pacific during northern winter. At peaks of the 11-yr solar activity, the increased ocean surface temperature increases evaporation, which intensifies the climatological precipitation maxima and associated upward motions, resulting in stronger trade winds, greater equatorial Pacific ocean upwelling and colder SSTs (or La Niña) events. This kind of "bottom-up" mechanism mainly considers only the role of the tropical Pacific played in climate due to ocean surface warming (cooling) in high (low) solar activity. Although the two categories of mechanism summarized in Gray et al. (2010) are important, they are not the fundamental mechanisms to form the atmospheric general circulations and climate and, therefore, seem to be the indirect mechanisms for the sun to influence climate change. To search for the fundamental mechanism in the sun-climate relationship is the goal of this research.

The present research results are presented in two parts. Part I provides a "bottom-up" atmospheric amplifying mechanism. It uses observational data analysis to validate the fundamental principles of climate dynamics by presenting different atmospheric circulation patterns and climate extremes for low and high solar activity. Part II (Weng, 2012) provides a nonlinear resonance mechanism of a climate system to the annual forcing modulated by multi-scale solar forcing. It is a combination of detecting the dominant timescales in decadal-centennial climate variability and a theoretical reasoning of the behavior of a simple forced dynamical system. Part I focuses on the mechanism why extreme climate events may be caused by extreme solar activity. Part II focuses on the mechanism why a similar extreme event in a given location may reoccur on various decadal-centennial timescales under the influence of a multi-scale cyclic external forcing. Part I is mainly for the spatial climate variability, while Part II is mainly for the temporal climate variability.

Before we proceed with our research in Part I on solar impacts on atmospheric circulations, we must go back to the basics first. There are mainly three kinds of thermal contrast driving the atmospheric general circulations on the assumption that the sun is invariant. When the sun is varying, these thermal contrasts would also be modified.

(1) Seasonal thermal contrast. Seasons are resulted from the yearly revolution of the earth around the sun and the tilt of the earth's axis relative to the plane of the earth's revolution. The elliptic shape of the rotation trajectory makes the earth in the boreal winter (austral summer) season be in the closest position to, and its axis tilts away, from the sun over a year. Thus, in the Northern Hemisphere, the winter general circulations would be more sensitive to a change in the TSI over a solar cycle than those in other seasons.

(2) Equator-to-pole thermal contrast. This latitudinal thermal contrast is the basic force to drive the three-cell meridional circulations in the troposphere: the direct Hadley cell and the polar cell, and the indi-

rect Ferrell cell in-between. The meridional temperature gradient determines the baroclinic unstable waves that directly related to weather activity (e.g., Lorenz, 1967). A major change in the meridional temperature gradient is essential to global climate change through changing such baroclinic wave activity (e.g., Lindzen, 1994). The high latitudes in winter are more sensitive than the tropics to a small change in the TSI over a solar cycle. When the sun is in its high (low) activity, the high-latitude surface receives more (less) solar radiation than normal, while the low-latitude surface does not change much. Thus, in general, the equator-to-pole temperature gradient and ultra-long wave activity should be reduced (enhanced) compared to the normal winter condition, which amplifies the solar forcing on extreme climate through these circulations and wave activity[b]. It should be kept in mind that the efficiency of the atmospheric heat engine depends on temperature difference between the tropics and the poles, not the globally averaged temperature itself. When the TSI is high (low), the earth as a whole receives more (less) solar incoming energy. The atmosphere as a "heat engine", however, may be less (more) efficient to transport heat from the tropics to the polar regions due to less (more) mid-latitude baroclinicity.

(3) Land-ocean thermal contrast. The difference in the heat capacity between land and ocean surfaces makes land be more sensitive than the oceans to a small change in incoming solar radiation over an annual cycle. When the TSI is varying over a solar cycle, land temperature may exhibit larger excursion due to its quicker response than the oceans (the latter may exhibit longer delayed response due to larger heat capacity and ocean mixing). Thus, when the sun is in its low (high) activity, the winter topographic waves affected by changed land-ocean thermal contrast would be enhanced (weakened).

Due to the above mentioned thermal contrasts on the earth surface, most sensitive region and season in the Northern Hemisphere surface to a change in the TSI should be in the high-latitude land during boreal winter. Thus, one of the direct thermal influences of solar activity could be seen in the strength and extent of the Siberian high over the massive high-latitude Eurasian land. The Siberian high is maintained by the radiative cooling over the massive bare land, associated with large-scale descending motion (e.g., Ding and Krishnamurti, 1987). It exerts great influences on the strength of the East Asian winter monsoon (EAWM) (e.g., Nakamura et al., 2002).

The increased baroclinicity in low solar activity favors ultra-longer waves to develop, because the dominant wavelength (wavenumber) of baroclinic waves is increased (decreased) as baroclinicity increases (e.g., Weng and Barcilon, 1988). As these solar influenced ultra-long waves reach the similar zonal scales of the solar enhanced stationary topographic waves, the baroclinic waves may resonate with the topographic waves and then greatly amplify. This is a favorable condition for blocking situation at the middle and high latitudes in the troposphere (e.g., Tung and Lindzen, 1979). The blocking situation may bring freezing wind equatorward from the polar areas and transport warm and moist air poleward from the tropics. This situation may also relate to southward shifted jets, warmer polar region and cooler middle latitudes in the Northern Hemisphere, resulting in a negative phase of the northern annular mode (NAM). The resonated and amplified baroclinic-topographic ultra-long waves propagate upward into the stratosphere, resulting in a favorable situation for the stratospheric sudden warming (SSW) in the high latitudes (e.g., Matsuno, 1971).

The winter situation during high solar activity can be very different due to reduced meridional temperature gradient, which favors relatively shorter ultra-long waves to develop. The stationary topographic waves are also weakened due to reduced land-ocean thermal contrast. The mid-latitude zonal flows are less wavy with less meridional heat exchange, resulting in the polar region that is colder than normal. Therefore, the atmospheric circulation patterns between the low and high activity can be very different. Such a difference results in different locations and strengths of the atmospheric centers of action and climate extremes between the low and high solar activity.

The "bottom-up" mechanism proposed here emphasizes the role of the atmospheric dynamics in the troposphere in the amplifying process of the climate response to a small change in solar radiation. Such a study on the solar variations directly forcing global surface temperature and climate was considered as the highest priority in the research of solar influences on global change (NRC, 1994).

The material of Part I is arranged as follows. Section 2 describes the date and methods used here. Section 3 analyzes the multi-scale solar variability and possible solar signals in the historic surface temperature data sets. Section 4 detects solar signals in the 3-D atmospheric circulations and compares their difference between extremely low and high solar activity.

[b]The surface reflection in the high latitudes than that in the low-latitudes is a feedback factor to enlarge the equator-to-pole temperature difference. When the sun is less (more) active than normal, the area of exposed or icy land surface and icy ocean surface may expand (shrink), so that the reflectivity of the surface for both land and ocean may be increased (decreased) in high latitudes, while little change in the reflectivity in low-latitudes where the underlying surface properties in both land and oceans are barely changed over a solar cycle.

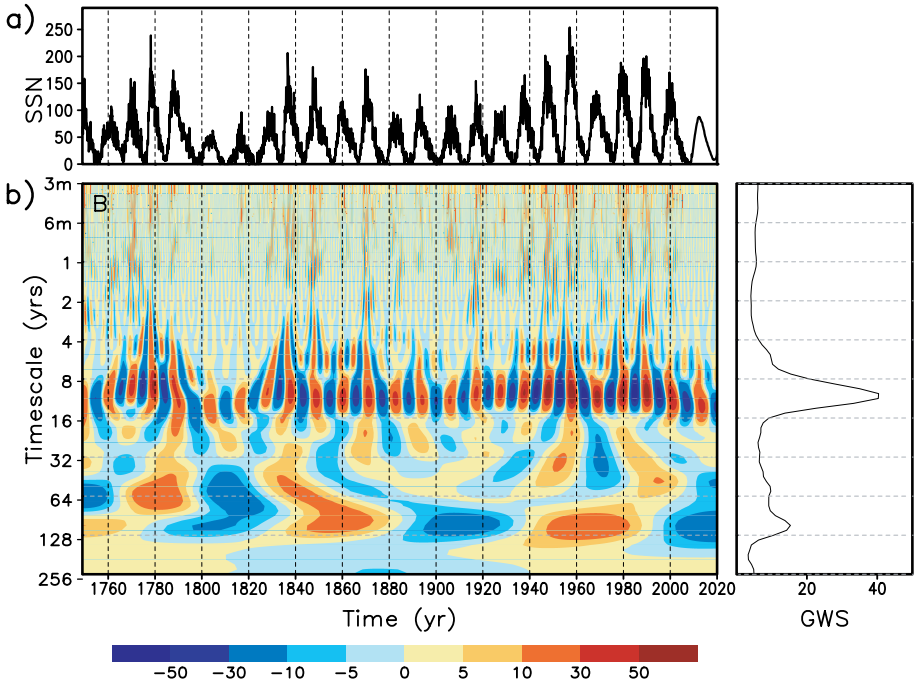

Fig. 1. (a) Time series of monthly-mean sunspot number (SSN) for the period of January 1749–December 2020 (predicted SSN after February 2011). (b) Corresponding real Morlet wavelet coefficients for timescales between three months and 256 yrs (left panel) and global wavelet spectrum (GWS; right panel).

Section 5 discusses possible relationship between solar activity and the ENSO cycle. Finally, section 6 summarizes and provides concluding remarks of Part I.

2. Data and methods

For the solar proxy, we use the monthly-mean sunspot number (SSN) for the period of January 1749–December 2020 (predicted after February 2011), from the US National Center for Geophysical Data.[c]

For the surface temperature, we use three sets of data in boreal winter (December-January-February). The 1° × 1° grid monthly-mean SST data for the period of January 1870–February 2011, the HadISST, are from the UK Meteorological Office (Rayner et al., 2003). The 5°× 5° grid historical monthly-mean land surface temperature anomaly data CRUTEM3v and the combined land/marine surface temperature anomaly data HadCRUT3v[d] (Brohan et al., 2006) for the period of January1850–February 2011, are also analyzed. Both anomaly data are the departures from the respective means of 1961–1990.

To study the plausible solar impacts on the atmospheric circulations, the 2.5°×2.5° grid monthly NCEP/NCAR Reanalysis data (Kalnay et al., 1996) (e.g., skin temperature, sea-level pressure, air temperature, geopotential height, wind, etc.) are used.

The seasonal mean of boreal winter is defined by the average of the monthly data of December, January, and February (DJF). All the data have been pre-processed to obtain their anomalies that are the departures from their respective means of 1961–1990. For convenience, we may neglect the word "anomaly" in the following analysis and discussion when a variable in focus is actually the variable's anomaly, unless specified otherwise.

In order to show different temporal behavior of the surface temperature variability between high and low latitudes, which could influence the temporal behavior of the mid-latitude temperature gradient, the complex Morlet wavelet (Weng and Lau, 1994) is used.

For each of the composites of solar minima (SCmin) and solar maxima (SCmax) on the 11-yr solar activity, six winters are chosen with a lag of couple of years. For SCmin, the winters are 1954/1955, 1965/1966, 1976/1977, 1986/1987, 1997/1998, and 2009/2010, and for SCmax 1948/1949, 1958/1959, 1970/1971, 1980/1981, 1989/1990 and 2002/2003.[e]

[c]ftp://ftp.ngdc.noaa.gov/STP/SOLAR_DATA/SUNSPOT_NUMBERS/INTERNATIONAL/monthly/MONTHLY, and ftp://ftp.ngdc.noaa.gov/STP/SOLAR_DATA/SUNSPOT_NUMBERS/INTERNATIONAL/prediction/sunspot.predict

[d]http://www.hadobs.org/

[e]The actual SCmin occurred in 1954.3, 1964.9, 1976.5, 1986.8, 1996.9, 2008.9, and SCmax in 1947.5, 1957.9, 1968.9, 1979.9, 1989.6, 2000.3, based on ftp://ftp.ngdc.noaa.gov/STP/SOLAR_DATA/SUNSPOT_NUMBERS/INTERNATIONAL/maxmin.

Such a delay of climate response to the 11-yr solar activity has been found in the analyses of earlier studies (e.g., White et al., 1997; Salby and Callaghan, 2004; Meehl et al., 2008; Roy and Haigh, 2010).

The observational data analyses presented and discussed here do not undergo any statistical significance test. Rather, we try to understand the results based on the principles of dynamical meteorology and climatology, based on which some speculations are provided for further research.

3. Solar signals in the historical surface temperature data

To detect solar signals at the surface temperature, we first compare the dominant timescales in the SSN and the surface temperature. Both the time series of the SSN (Fig. 1a) and its wavelet coefficients (Fig. 1b) show that the 11-yr solar activity is dominant yet nonstationary, which cycle-length and intensity varies with time on multi-scale longer timescales. Besides, there is the Gleissberg cycle (Gleissberg, 1965) peaked around 80–90 yrs, which is dominant over the interdecadal-centennial timescale band, and has greatly enhanced since the early 20th century (Fig. 1b). If the predicted SSN for Solar Cycle 24 is largely correct, the negative phase of the current Gleissberg cycle might hit its minimum around 2020. Moreover, a 60-yr signal in the SSN, which is stronger than the 80–90-yr signal in the earlier data period, is barely discernable since the early 20th century. As a result, the 60-yr solar signal is much weaker than the 90-yr solar signal in the global wavelet spectrum.

Figure 2a presents the zonal-mean temperature, which shows apparent warming trend over the 20th century at most latitudes, especially in the northern high latitudes. Also shown in Fig. 2 are low-passed ($>$ 8 yrs) time series of the mean temperature for the high latitudes (52.5°–67.5°N) (Fig. 2b) and low latitudes (22.5°–37.5°N) (Fig. 2c), which exhibit apparent decadal variability with long-term variation that basically correspond to the intensity variation of the 11-yr solar cycle. As explained in the introduction, the excursion of the change in temperature at high latitudes is indeed much larger than that at low latitudes. The difference in temperature between the low and high latitudes (Fig. 2d) may represent the meridional (latitudinal) temperature gradient for the mid latitudes centered at 45°N. Apparently, the temperature gradient largely depends on the high-latitude temperature, so that the long-term variation tendency in Figs. 2b and 2d are basically opposite.

The detailed temporal characteristics of the three time series in Fig. 2 are better seen in the wavelet domain (Fig. 3). The high-latitude temperature (Fig. 3a) is predominated on the interannual timescales, especially the QBO timescale. The decadal signal is buried in the broadband spectrum. It might be due to the fact that the intensity and cycle-length of the decadal signal exhibits a large modulation on longer timescales so that in the global wavelet spectrum the decadal signal is smeared. However, the 88-yr signal stands out clearly over the interdecadal-centennial timescale band, with a secondary signal whose cycle-length is about double of the 88-yr timescale. As expected, the low-latitude temperature (Fig. 3b) exhibits much less

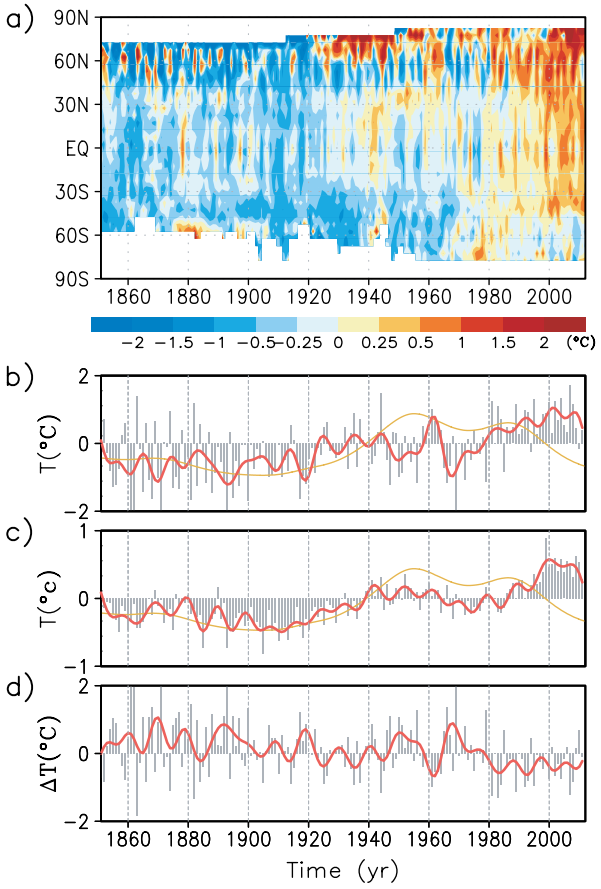

Fig. 2. (a) Zonal-mean HadCRUt3v temperature anomaly (with respect to the mean of 1961–1990) for the winters of 1850/1851–2010/2011. (b) and (c) are the time series of the zonal-mean temperature anomaly averaged over high latitudes (52.5°–67.5°N) and low latitudes (22.5°–37.5°N), respectively. The bars in (b) and (c) are for individual winters, the red curves are the low-pass (>8 yrs) time series, and the orange curves are the intensity of the 11-yr SSN. (d) Latitudinal temperature gradient in the mid-latitudes (ΔT), which is the difference of (c) and (b), namely, (c)−(b). Note that the temperature range used in (c) is different from that used in (b) and (d).

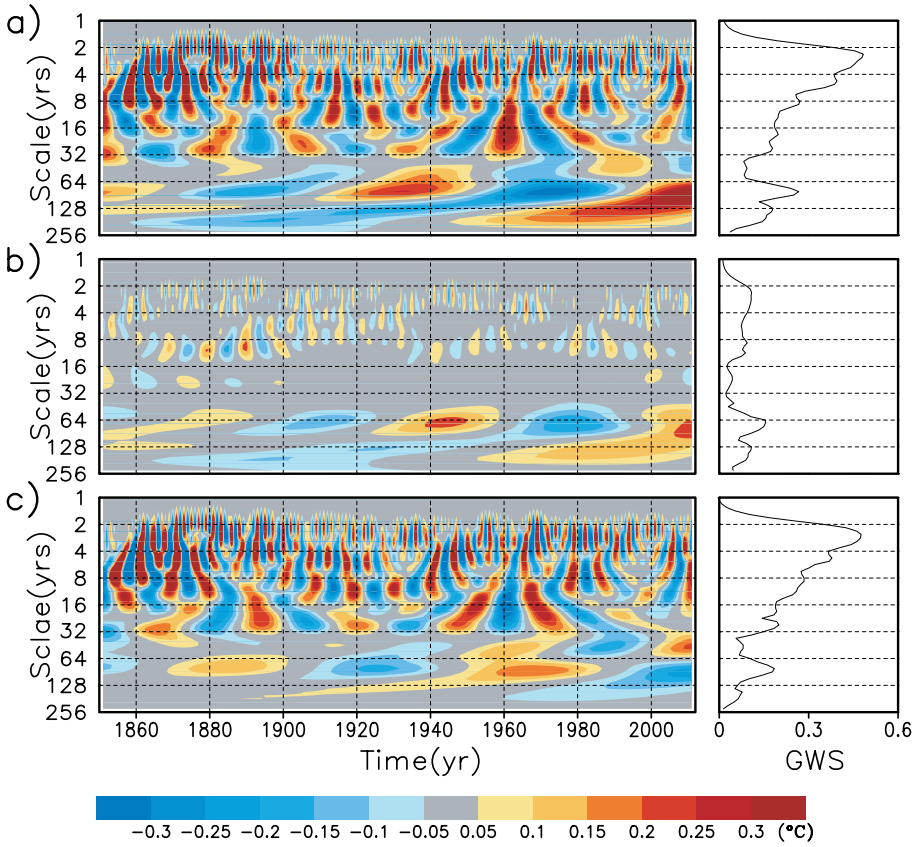

Fig. 3. Real wavelet coefficients (left panels) and the GWS (right panels) of the three temperature anomaly time series shown in Figs. 2b–d. (a) High latitudes, (b) low latitudes, and (c) ΔT.

variance compared to the high-latitudes. It is interesting that the 60-yr timescale predominates over the whole global wavelet spectrum. This timescale is similar to the predominant timescale of the AMO. Since the change in the meridional temperature gradient is largely contributed by the change in the high-latitude temperature, on the interdecadal-centennial timescale, the meridional temperature gradient in Fig. 3c is basically out of phase with the temperature in the high latitude in Fig. 3a. The decades of global warming/cooling periods correspond to high/low solar activity on the interdecadal-centennial timescales (Fig. 1b). Thus, during the global warming/cooling periods, the meridional temperature gradient is very likely to decrease/increase with some delay, implying a decreased/increased baroclinic long wave activity in the mid-latitude troposphere.

Since the data record is too short to make any solid conclusion here, we can only speculate that the currently decreased meridional temperature gradient might increase as the SSN marches towards the coming minimum of the Gleissberg cycle. It implies that the ultra-long waves, which closely related to the blocking situation and persistent extreme weather/climate events, might be more active during this period. This speculated mechanism will be studied with atmospheric data in the next section.

During the 20th century when the 60-yr solar signal is hardly discernable some climate variables, such as the Atlantic Multidecadal Oscillation (AMO) exhibits a dominant variability on the 60-yr timescale (e.g., Kerr et al., 2000; Semenov et al., 2010; Weng, 2012). The inconsistency between the dominant timescales in solar activity and some climate variables is an interesting issue in the debate on the sun-climate relationship. A possible solar origin of the 60-yr climate variability will be explored in Part II.

4. Solar signals in the atmospheric circulations

4.1 *Interannual to interdecadal atmospheric variability*

In many studies on "global warming", the "global mean" surface temperature data are often used. Figure 4 shows how the air temperature in the "global mean"

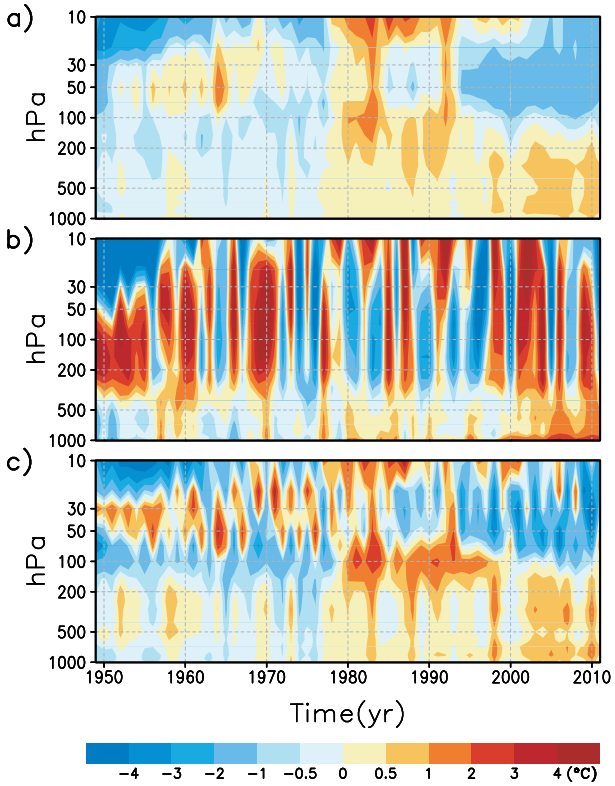

Fig. 4. Zonally averaged air temperature anomalies for (a) the global mean (90°S–90°N), (b) the northern polar region (65°–90°N), and (c) the tropics (5°S–5°N).

and those in the regional means may vary differently with time and height. During the data period, the "global mean" air temperature at 1000 hPa does show a warming trend with a "regime shift" in the late 1970s, which has been confirmed by many previous studies (IPCC, 2007, and the references herein). On the top of that trend, there are ups and downs on shorter timescales. The variability of the air temperature in the stratosphere is rather complicated. If only the data back to the late 1970s were used, a global cooling trend in the stratosphere existed, corresponding well to the global warming trend in the underneath troposphere. However, such a stratospheric cooling trend does not hold in the data period of six decades. The stratospheric air temperature exhibits different temporal features on different timescales at different levels from those in the surface temperature. Thus, the relationship between the stratosphere and troposphere, which influences the surface temperature, is not simple. This is a piece of evidence that the "top-down" mechanisms of solar impacts on the surface temperature through the mid-atmosphere may only play indirect and non-fundamental roles.

In the zonal air temperature averaged over the northern polar region (65°–90°N) (Fig. 4b), except for the lower troposphere that shows a warming trend with more warming than that in the global mean temperature in Fig. 4a, the upper troposphere and most of the stratosphere exhibit quite strong interannual signal. The vertical extent of such interannual variability up to 10 hPa changes greatly. The interannual variability, modulated on the interdecadal timescales, in the polar region is more apparent than in the global mean air temperature.

The zonal mean air temperature at the tropics (5°S–5°N) (Fig. 4c) exhibits very different temporal features from those in the polar region (Fig. 4b). The warming trend, in a lesser degree than that in the lower troposphere temperature in Fig. 4b, is seen from the surface to upper troposphere with a regime shift at the late 1970s. An apparent difference between Figs. 4b and 4c is that the interannual variabilities in the polar region have longer timescales than those in the tropics. This kind of difference in timescale may be understood by different responses of the climate variables in different latitudes to different annual forcing even without impact of solar activity (Jin et al., 1996). This result provides a hint that linear analysis (correlation/regression) relating the temperature variability in the tropics and that in the higher latitudes may result in misleading information due to the fact that their variabilities are not on the same timescale even in the same broad category of the "interannual variability".

There are two warm events in the stratosphere in all the three panels in Fig. 4, which are a couple of years after the two SCmax in 1980 (Cycle 21) and 1989 (Cycle 22). These stratospheric warming events have previously been related to the 1982 El Chichón eruption in Mexico and the 1991 Pinatubo eruption in the Philippines. The climate impacts of volcanic eruptions are such that the volcanic aerosols cool the earth surface but heat the stratosphere (Robock, 2002). However, the abrupt surface cooling after these two eruptions in Fig. 4a is not apparent. The zonal mean temperature in Fig. 4 shows that the stratospheric warming at 10 hPa in the 1980s, while oscillating on a QBO timescale, occurred even before the El Chichón volcanic eruption. It is known that in the layer between 100–10 hPa (about 15–35 km), there is a layer of ozone that absorbs solar short wave (at the UV wavelength) that also warms up the stratosphere, especially in the tropics where photochemical process is stronger than other regions (e.g., Shindell et al, 1999). Moreover, the warming in the high latitudes (Fig. 4b) is much stronger than that in the tropics (Fig. 4c), while the locations of the two volcano eruption are more close to the tropics than to the high latitudes. The fact that the two stratospheric warming periods started before

or the same winter of the two volcanic eruptions, and that the high latitudes has larger warm anomaly than the tropics show that the stratospheric warming in the 1980s and the early 1990s could be more influenced by the high solar activity than the effects of the volcanic eruptions during those periods.

The temperature variability is closely related to zonal wind variability in space and time. Figure 5 presents zonally averaged zonal wind for three latitude belts: the high latitudes (65°–90°N) (Fig. 5a), the middle latitudes (30°–60°N) (Fig. 5b), and the tropics (5°S–5°N) (Fig. 5c). From the high latitudes to the tropics, the pressure-time structure of the zonal wind becomes more complex with more vertical nodes of phase change between the westerlies and the easterlies on the interannual timescales. The mid-latitude wind exhibits shift from mainly the easterlies to mainly the westerlies in the late 1970s, corresponding to the global temperature shift from cold to warm at the same time (Fig. 5a). Such a shift largely corresponds to the change in solar activity from low to high on the combination of a couple of interdecadal timescales (Weng, 2005). The fact that the zonal wind in different latitudes exhibit different temporal characteristics also implies that linear analysis tools are not sufficient to obtain a good understanding of the relationship between climate variables in one region and those in other regions, unless the variables in different regions vary on the same timescales.

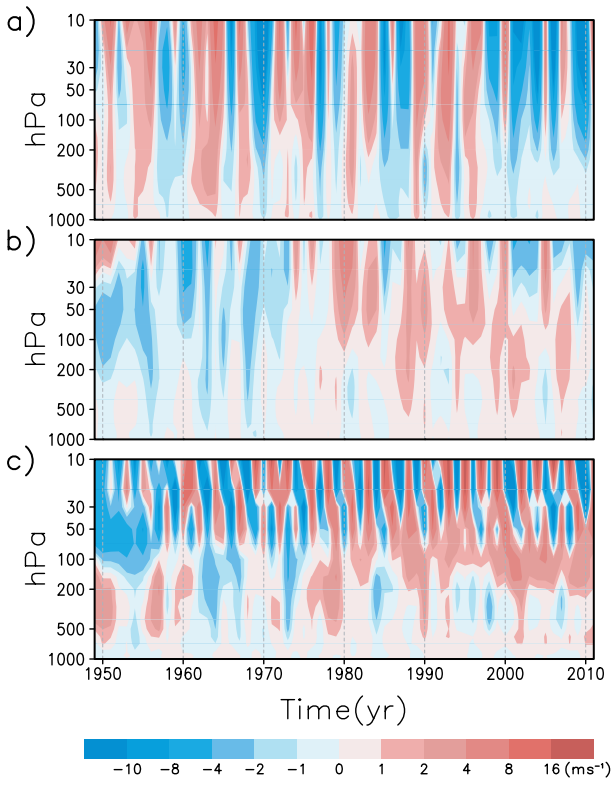

Fig. 5. Variations of the zonally averaged zonal wind anomalies with time and pressure height in (a) the high latitudes (65°–90°N), (b) the mid latitudes (30°–60°N) and (c) the tropics (5°S–5°N).

Keeping the caveat in mind, in the following subsection, we use composites to seek for the 11-yr solar signal in the atmospheric circulations, even though the composites may not completely remove the influence from the interannual and interdecadal variability.

4.2 *Atmospheric circulation patterns modified by the 11-yr solar activity*

Based on the six winters for each of SCmin and SCmax, as given in section 2, this subsection presents the corresponding general circulation patterns. The goal is to see whether these patterns are consistent with the idealized features as speculated based on the principles of atmospheric dynamics in the Introduction when the TSI is extremely low or high over the 11-yr solar activity.

4.2.1 *Surface temperature and centers of actions*

Figure 6 compares the skin temperature and sea-level pressure (SLP) climatology (Fig. 6a) with the composites of their corresponding anomalies for SCmin (Fig. 6b) and SCmax (Fig. 6c).

In Fig. 6a, there are several centers of action in the Northern Hemisphere winter. The strongest and the largest one is the Siberian high, which is an intense cold anticyclone. It is a shallow cold-core system confined to the lower troposphere below 500 hPa, and is the main cause of frequent cold outbreaks over eastern Asia (e.g., Gong and Ho, 2002). The Greenland high is in the region from Greenland ice sheet to the northeastern Canada. The North American high has much less spatial scale and strength than the Siberian high.

In the middle and high latitudes, there are two large-scale low-pressure systems, which are major weather makers in the latitude belt. The Aleutian low, centered near the Aleutian Islands, and the Icelandic low, centered between Iceland and Greenland, are the two major sources of many strong cyclones. As other cyclones approach these two semi-permanent air masses from the west, they slow down and intensify, which results in extended periods of stormy, unsettled weather in the regions. As will be shown later, these two low regions correspond to the two storm tracks in Northern Pacific and North Atlantic in the mid-troposphere.

In the subtropics, there are weak subtropical anticyclones. One is the North Pacific high, located in the northeast of Hawaii. Another is the North Atlantic

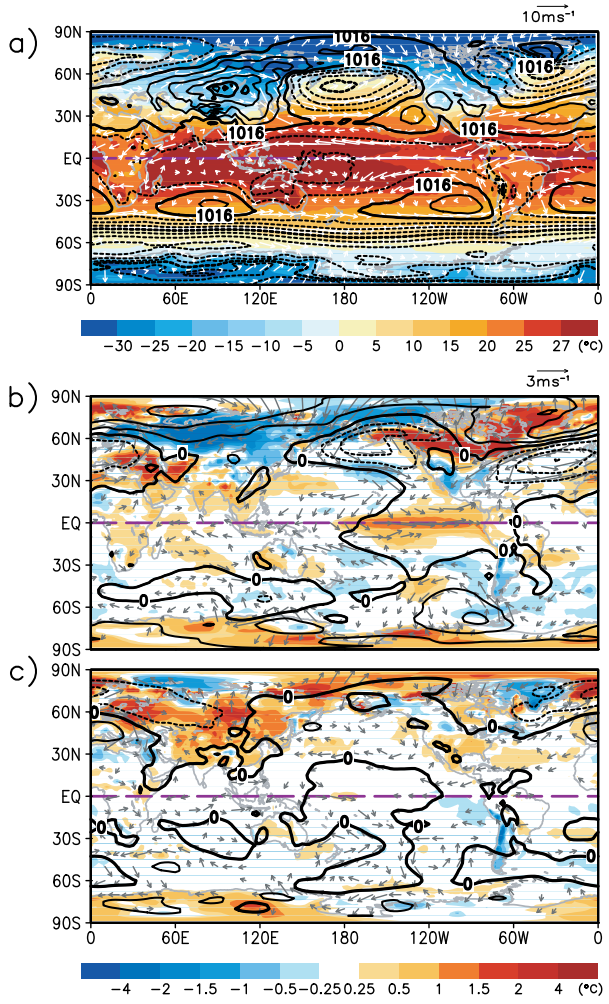

Fig. 6. Skin temperature (shaded), SLP (contours) and 850-hPa wind for (a) 1961–1990 mean, and the anomaly composites for (b) six SCmin and (c) six SCmax. The contour interval in (a) is 4 hPa, and in (b) and (c) is 2 hPa. The wind vectors with magnitude less than 0.5 m s^{-1} have been neglected.

high, which is also named as Azores high or Bermuda high. Both subtropical highs are weak in winter season.

The Azores high and the Iceland low form a south-north dipole pattern known as the North Atlantic Oscillation (NAO). The NAO is an important component of the Northern Annular Mode (NAM; or sometimes called Arctic Oscillation, AO). The NAM/AO consists of a dipole between the polar cap region and the surrounding zonal ring centered along 45°N. The variability of the NAM has great impacts on the weather in the Northern Hemisphere (e.g., Wallace and Thompson, 2002; Li and Wang, 2003). The NAM is an integration of the change in the strength and location of these centers of action and the moving lows (cyclones) and highs (anticyclones) that are directly related to regional weather events. Therefore, to explore the solar impacts on climate, we should study how a change in the TSI over a solar cycle may affect atmospheric circulations and wave activity that modify the strength and location of these centers of action. It is the first step to understand the "bottom-up" amplifying mechanism of solar impacts on climate change.

The difference of the skin temperature and SLP anomaly patterns between Fig. 6b (SCmin) and Fig. 6c (SCmax) is apparent even by eye. First, the surface in the Northern Hemisphere at large is cooler for SCmin and warmer for SCmax than the climatology. Such a difference is especially prominent in much of the land surface temperature. Second, the waves in the middle to high latitudes for SCmin are more active than those for SCmax. The waves for SCmin have longer wavelength (or zonal scale), larger south-north excursion (meridional scale), and larger amplitude (intensity) than those for SCmax. These differences are consistent with the dynamical principles mentioned in the Introduction. The meridional temperature gradient and, therefore, the baroclinicity in the middle latitudes look stronger for SCmin than SCmax. The data presented here is for the seasonal mean, so that what we see here is the averaged circulation patterns of the six winters for each case.

Among the solar modified centers of action, the most prominent feature is that the Siberian high is colder and enhanced for SCmin when the vast Eurasian land surface receives less solar radiation (Fig. 6b), while warmer and weakened for SCmax when the land receives more solar radiation (Fig. 6c). Such a contrast of the Eurasian land surface temperature between SCmin and SCmax is further enhanced by land-atmosphere radiation-dynamic feedback processes as mentioned in footnote b. This amplifying mechanism cannot be simply estimated by the magnitude of the solar radiation change over solar cycles when the solar forcing is compared with other external radiation forcings that do not influence the surface temperature and circulation patterns in the same way as the solar radiation does.

A paradox in the patterns of SCmin (Fig. 6b) is that the surface temperature anomalies in much of the land in Canada and Greenland are positive instead of negative for SCmin, which cannot be explained by reduced solar radiation received at the land surface for SCmin as the case of the Siberian high. This paradox might be understood by atmospheric dynamics. The high pressure system over Siberia brought frigid arctic air to its south and southwest along the eastern frank of the giant anticyclonic system over the Eurasian continent. Then, the air continues to move westwards into

northern Europe. Meanwhile, a part of the air flow on the western frank of the Siberian high as warm and moist southerly winds going north to the west of Iceland, passing over the warm ocean surface. This is a typical situation of a high-latitude high pressure system in winter: to the east (front) of the high system there is a cold anomaly region; to the west (rear) there is a warm anomaly region. Due to thermo-dynamical processes, the more extensive and intensive a high system is, the larger temperature contrast between the front and rear regions of the system would be. Greenland is mainly covered by ice sheet. For SCmin, when the Siberian area is colder than normal winters due to reduced solar incoming radiation, Greenland temperature, due to its ice sheet cover, would not reduce as much as the Siberian area does. Thus, in Greenland, the thermal effect due to low solar activity may not be overcome the warm dynamical effect by flows originated from the Siberian high. For SCmin, such a phenomenon might occur when the zonal flow is dominated by wave-one over the high-latitudes. If the zonal flow is dominated by wave-two, the situation would be different.

The expanded Siberian high for SCmin also pushes the Aleutian low moving southeastward while it intensifies in the Gulf of Alaska and off the west coast of northern North America. Meanwhile, the Icelandic low also shifts southward. The two low systems and the Greenland high may form a blocking situation in the middle and high latitudes. Such a blocking situation may affect weather patterns in the region greatly. Unlike normal pressure cells which drift around the globe led by the prevailing westerlies of the upper atmosphere, the blocking highs are capable of remaining more or less stationary for weeks, resulting in constant cold breaks in the front region, while warm spells in the rear region, of blocking highs. In the tropical Pacific, the surface temperature and the 850-hPa wind fields exhibit an El Niño-like condition.

For SCmax (Fig. 6c), the most striking feature in the middle and high latitudes is the large-scale temperature pattern with opposite anomaly sign to that for SCmin. The warm anomalies are in Eurasia and in the region from the eastern Siberia to Alaska, while Greenland exhibits cold anomaly. The strength of the winter centers of actions is in general weakened, especially the Siberian high where negative SLP anomalies prevail and the Aleutian low where positive SLP anomalies are found. In the tropical Pacific, the temperature and wind anomalies indicate a weak La Niña-like condition.

Although the change in the TSI over an 11-yr solar cycle is only about 0.1%, the change in the surface temperature in some regions between the composite low and high solar activity could be quite large. For example, the mean winter temperature in the large Siberian area (50°–70°N, 80°–110°E) averaged over the data period is −21.80°C, with the standard deviation (σ) 2.66°C. The composite temperature anomalies for SCmin and SCmax are −1.78°C and +1.41°C, respectively. The temperature anomalies for the 2009/2010 and 2010/2011 winters are −4.80°C (-1.77σ) and −2.06°C (-0.76σ), respectively. While both winters are related to SCmin, the 2009/2010 winter (during an El Niña event), seems to be more influenced than the 2010/2011 winter (during a La Niña event) by the abnormal SCmin between Solar Cycle 23 and Solar Cycle 24.

In summary, the winter climate conditions represented by the surface temperature and SLP are enhanced a couple of winters after SCmin while weakened after SCmax. Thus, an extremely low (high) solar activity may give a hint that more (less) extremely cold events are likely to occur in the middle latitudes in the following couple of winters, and/or less (more) cold spells are likely to occur in the high latitudes.

4.2.2 *General circulations in the mid-troposphere*

The 500-hPa geopotential height and omega (vertical pressure velocity) patterns for the 1961–1990 means and the anomaly patterns related to SCmin and SCmax are presented in Fig. 7. In the Northern Hemisphere, the 30-yr winter climatology shows that the polar vortex in the mid-troposphere is eccentric toward the region between North America and Greenland, with a deep trough extending to the eastern Siberia. The two major mid-troposphere troughs of the westerlies correspond to two large-scale descending regions over the central Siberia and North America, bringing cold air from the polar region in the rear of the troughs. Meanwhile, two major large-scale ascending regions in the front of the troughs correspond to two extratropical storm tracks. These storm tracks extend from the westernmost parts of the Pacific and Atlantic, where the large temperature contrast between land and oceans surface favors the cyclonegenesis that brings weather events. The location and strength of the mid-troposphere mid-latitude storm tracks are basically determined by the equator-pole and land-ocean thermal contrasts and change over an annual cycle when these thermal contrasts change. It is natural to speculate that the location and the strength of the storm track will and must be affected by the change in the TSI over solar activity cycles. Therefore, to compare the influence of SCmin and SCmax on the location and strength of these mid-latitude storm tracks, as well as the accompanied regions with ascending/descending air, will have important impli-

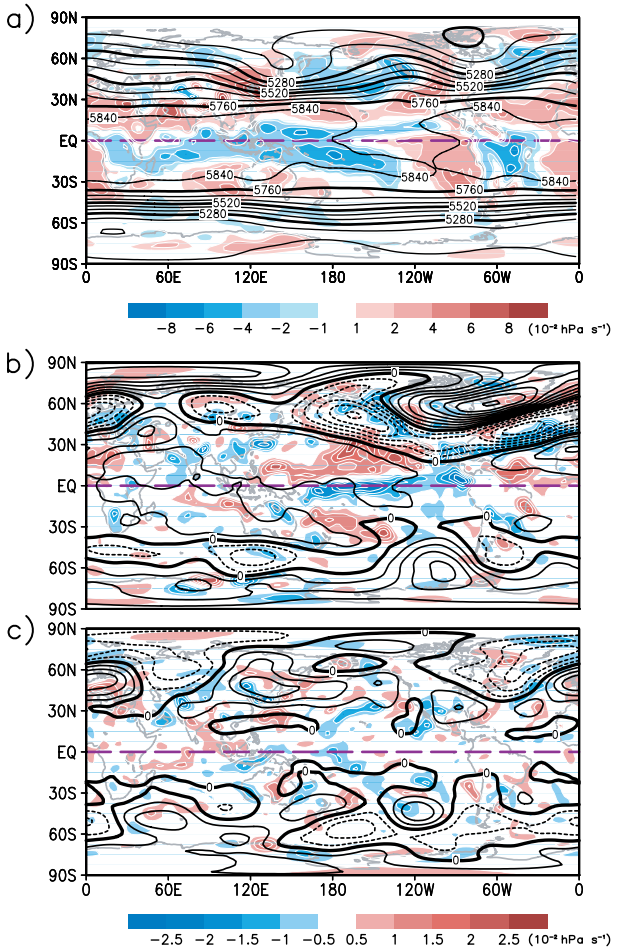

Fig. 7. Omega (shaded) and geopotential height (contours) at 500 hPa for (a) 1961–1990 mean, and the anomaly composites for (b) six SCmin, and (c) six SCmax. The contour interval in (b) and (c) is 10 m.

cation in improve prediction of when and where large-scale floods and droughts may occur.

For SCmin (Fig. 7b), the polar region is mainly occupied by positive geopotential height anomalies, implying a weakened polar vortex. Several negative anomaly centers almost form a negative anomaly belt over the mid latitudes. The storm tracks over the northeastern Pacific and northern Atlantic shift equator-ward. This mid-troposphere circulation pattern may greatly change the normal pattern of vertical velocity in Fig. 7a, and favors a blocking situation near the surface to develop as implied in Fig. 6b. As indicated earlier, the location and strength of a blocking situation is directly related to the region and severity of extreme weather/climate events.

For SCmax (Fig. 7c), the polar region is mainly occupied by negative anomalies, implying an enhanced polar vortex. Positive anomalies are over the Siberian area. Storm tracks shift pole-ward. However, the geopotential situation is not just a simple phase reverse from that in Fig. 7b. Such a mid-troposphere circulation condition may not favor the development of persistence of large-scale blocking situation near the surface.

4.2.3 *Zonal circulations in the Tropics and northern polar region*

To further show the difference of the tropical circulations between SCmin and SCmax, we present the air temperature, zonal wind and the Walker cells for SCmin (Fig. 8b) and SCmax (Fig. 8c) with regard to their climatology (Fig. 8a). The normal Walker cells in Fig. 8a exhibit large-scale ascending flow in the western tropical Pacific. A large part of the ascending flow turns to west toward the Indian Ocean as easterlies. Another part of the ascending turns to east and descends in the eastern tropical Pacific. The eastern troposphere is dominated by the easterlies, while the western troposphere is dominated by the westerlies.

The most apparent difference between Figs. 8b and

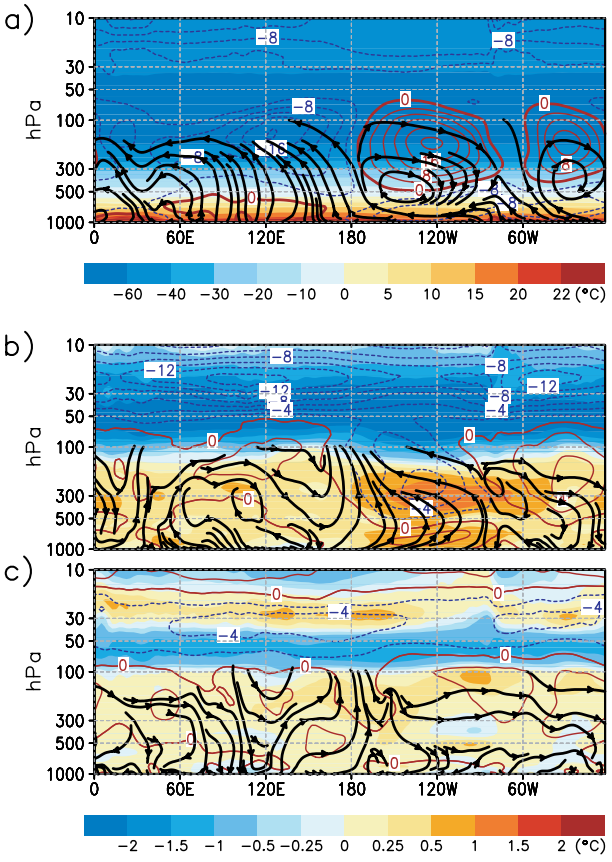

Fig. 8. Tropical (5°S–5°N) air temperature (shaded), zonal wind (red and blue contours for westerlies and easterlies, respectively), Walker cells (streams) for (a) the 1961–1990 mean, and the anomaly composites for (b) six SCmin and (c) six SCmax. The contour interval in (a) is 4 m s^{-1}, and in (b) and (c) is 2 m s^{-1}.

8c is in the stratospheric air temperature. For SCmin (Fig. 8b), there is a deep cold belt around the globe between 100–10 hPa, with the coldest layer centered near 50 hPa. For SCmax (Fig. 8c), a warm belt is found in the layer of 40–20 hPa. The ozone layer in the lower stratosphere absorbs the sun's ultraviolet radiation in the TSI.[f] Thus, the decrease/increase in the TSI would decrease/increase the air temperature in the lower stratosphere for SCmin/SCmax compared to the climatology. This is an influence of solar activity on the stratosphere, an important factor in the "top-down" mechanism (e.g., Haigh, 2007; Gray et al., 2010). In Fig. 8c, the normal easterlies above 20 hPa is decreased by the westerly anomalies above the layer of the warm belt.

The temperature in the troposphere does not seem to have a significant difference between SCmin and SCmax, except that large warm anomalies over the Niño3 region (5°S–5°N, 150°–90°W) for SCmin. The largest warming is found in the upper troposphere, where the warm anomaly is mainly due to latent heat release in the ascending flow. The anomalous easterlies center accompanied the warm center in the upper troposphere shows that the main Walker cell in the tropical Pacific is greatly modified by El Niño events. For SCmax, there is cold anomaly in the eastern tropical Pacific and the Indian Ocean. However, the cold anomalies are relatively weak. Figure 8 shows that the temperature and wind anomalies in the tropics exhibit less vertical nodes for SCmin than SCmax.

Figure 9 shows the counterparts of Fig. 8 for the high-latitudes. For SCmin (Fig. 9b), the lower troposphere in the eastern hemisphere is colder while that in the western hemisphere is warmer, which correspond well to the skin temperature anomalies seen in Fig. 7b. Large-scale intensive stratospheric warm anomaly is mainly seen between 60°E–60°W with higher location over Siberia than over Canada-Greenland. Meantime, the stratospheric polar vortex is weaker due to the anomalous easterlies. Such a large-scale intensive stratospheric warm anomaly is not seen for SCmax (Fig. 9c). Figure 9 implies that SCmin may favor more occurrence of the SSW events than SCmax does, and the warming seems to have a combination of wave-one and wave-two. It is consistent with the dynamical principles explained in the Introduction.

4.2.4 *Meridional circulations*

A classic three-cell meridional circulation pattern is seen in Fig. 10a for the climatology over the 30 years. Much of the ascending branch of the Hadley cell is located to the south of the Equator. Its descending branch is over the subtropical region centered near 30°N where droughts prevail. The ascending branch of the polar cell is centered near 60°N, with the descending branch over the polar region north of 70°N. The thermally indirect Ferrell cell is in between the two thermally direct cells. In the Northern Hemisphere, the subtropical jet is over the 30°N near 250 hPa. The polar jet is over north of 60°N with the strongest westerlies above 10 hPa. The tropical easterlies have the least meridional extent at the upper troposphere. These meridional circulations seem to be greatly modified by solar activity.

For SCmin (Fig. 10b), the descending branch of the polar cell expands equatorward at least by 10 degrees to 60°N, where it is occupied by ascending flow in the normal winters. The ascending branch over the mid-latitudes has also moved equatorward to the south of 30°N. The wide latitude range between 30°N and 60°N with anomalous updraft, which include the descending branch of the Ferrell cell in Fig. 10a, is now the region where the weather related baroclinic waves are more active than usual. The ascending branch of the Hadley cell near the equator is enhanced, yet its meridional extent is reduced, so that the subsidence between 15°–30°N is enhanced, compared to the climatology. It implies that severe droughts may occur in this latitude belt. The southern part of the climatological dried region in the North Hemisphere may get even drier. The meridional extents of the anomalous three cells, except for the descending region of the polar cell, are all look squeezed. Since the heat source is in the tropics and the heat sink in the polar region in the Northern Hemisphere, the enhanced equatorial updraft and polar downdraft in Fig. 10b implies that the atmospheric "heat engine", which transport heat from the tropics to polar region by the meridional circulations in the Northern Hemisphere, is enhanced in Fig. 10b for SCmin. The enhanced heat engine is due to enhanced meridional temperature gradient and, therefore, more wave activity and poleward heat transfer for SCmin as explained in Introduction.

The most intriguing feature in the stratosphere is the polar warming centered near 70 hPa, as seen in Fig. 10b. There are stratospheric cooling and tropospheric warming over the tropics and subtopics, respectively. Such a temperature anomaly distribution corresponds to a sandwich-like wind anomaly in Northern Hemisphere: the easterlies over the pole and tropics-subtropics, while the westerlies over the mid-latitudes. The easterly phase of the tropical stratospheric QBO seems to be favored by SCmin. The easterlies over the high-latitudes and westerlies over the mid-latitudes imply a weakened polar vortex, corresponding to negative phase of NAM/AO, and a nar-

[f] http://en.wikipedia.org/wiki/Ozone_layer

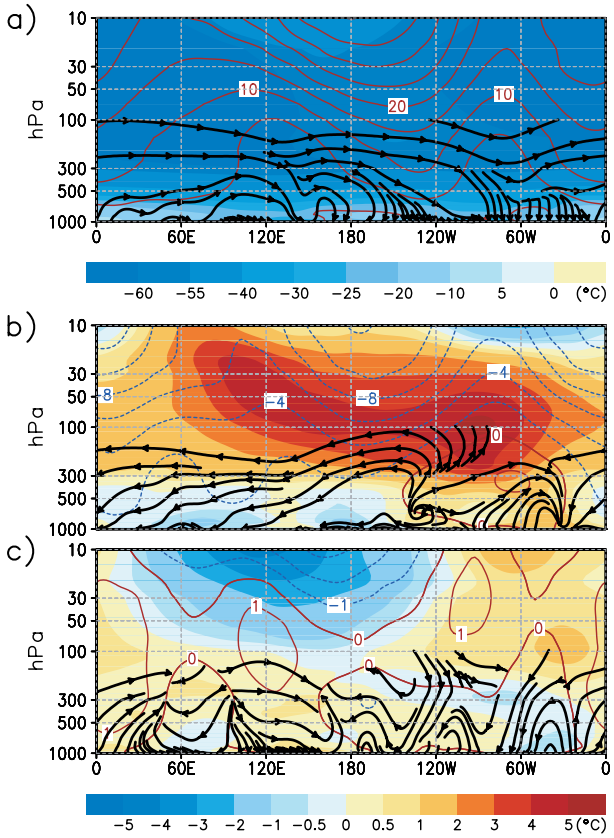

Fig. 9. Same as Fig. 8, except for the polar latitude belt of 65°–90°N.

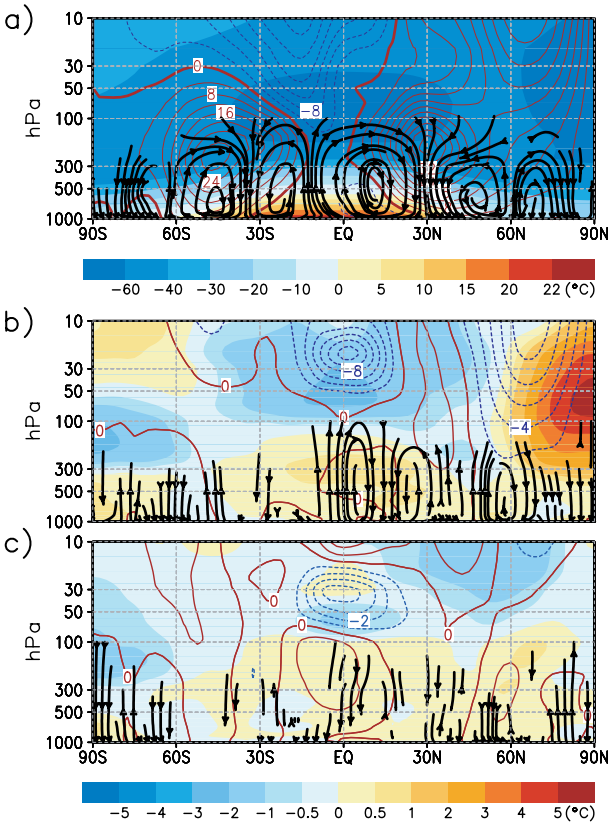

Fig. 10. Zonally averaged air temperature (shaded), zonal wind (red and blue contours for westerlies and easterlies, respectively), meridional circulation (streams) for (a) the 1961–1990 mean, and the anomaly composites for (b) six SCmin and (c) six SCmax. The contour interval in (a) is 4 m s^{-1}, in (b) is 2 m s^{-1}, and in (c) is 1 m s^{-1}.

rowed yet enhanced and equator-shift subtropical jet.

For SCmax (Fig. 10c), the anomalous meridional cells are not as apparent as those for SCmin. In the Northern Hemisphere, there is anomalous downdraft over the tropics and updraft over the polar region. It implied that the anomalous atmospheric "heat engine" in Fig. 10c is reversed from that in Fig. 10b, so that the atmospheric heat engine is weakened for SCmax. The weakened heat engine is due to reduced meridional temperature gradient and, therefore, less wave activity and poleward heat transfer, which is largely opposite to the condition for SCmin yet asymmetric about the climatological condition. The conditions between SCmax and SCmin composites are not anti-symmetric, especially over the stratospheric polar region, where the circulation could be greatly influenced by the far tropical stratospheric QBO that is modulated by solar activity (e.g., Labitzke and Loon, 1988; Salby and Callaghan, 2004; Camp and Tung, 2007).

To further show the difference of the meridional circulations between low and high solar activity on the interdecadal timescales, the time series of the NAM index is presented in Fig. 11. The similar feature on the 11-yr timescale is also seen on the interdecadal timescales. That is, when the solar activity is low (high), the NAM index tends to be negative (positive) on the interdecadal timescales. The NAM index was basically higher in the past three decades than the previous three decades, corresponding well to the SSN variability on the interdecadal timescales. At the present, the NAM seems to enter another few decades that might largely be negative since the SSN on the Gleissberg timescale has entered a negative phase based on recent decreased trend in SSN.

The time series of the zonally averaged meridional divergence at the mid-latitudes surface is presented in Fig. 12, which also links the meridional circulation to the change in the SSN on the interdecadal timescales. As the solar activity is low (high), the mid-latitude surface is largely controlled by convergent (divergent) meridional winds. This is due to the enhanced (reduced) wave activity for SCmin (SCmax). Thus, it is understandable that there would be more ascending (descending) air flow in the lower to middle troposphere in the mid-latitudes during low (high) solar

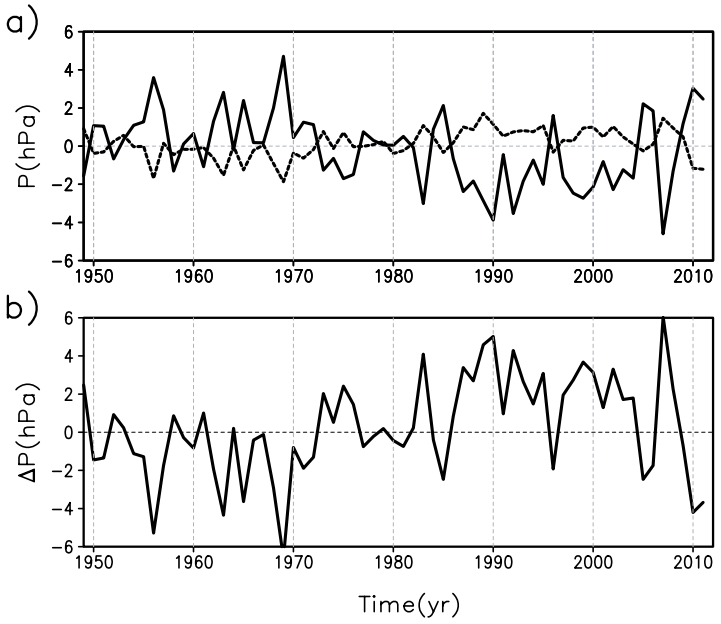

Fig. 11. (a) Zonally averaged SLP anomaly in the middle to high latitudes ($P_{\rm high}$, 55°–65°N, solid line) and the low latitudes ($P_{\rm low}$, 20°–30°N, dashed line). (b) $\Delta P = P_{\rm low}$–$P_{\rm high}$, as an index for the Northern Annular Mode (NAM).

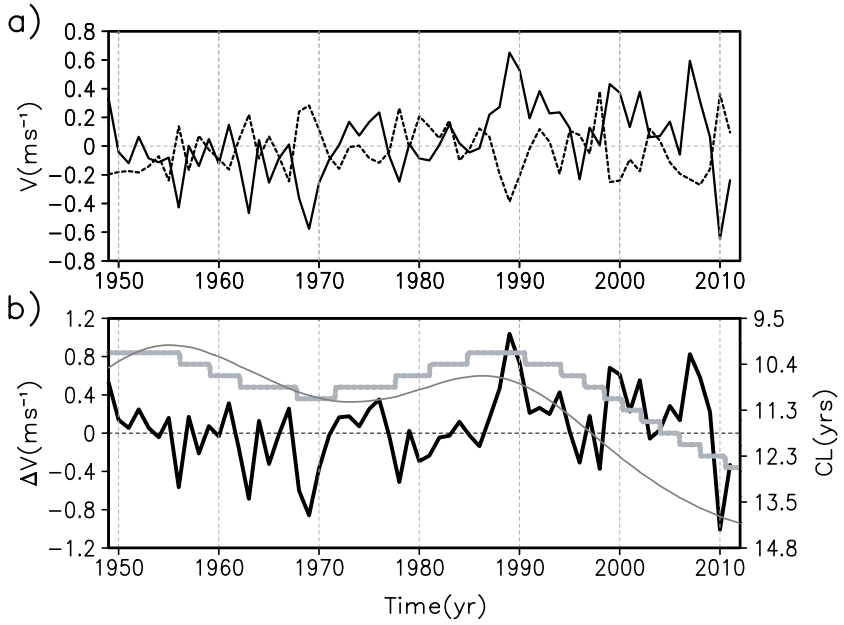

Fig. 12. (a) Zonally averaged surface meridional wind anomaly in the middle to high latitudes ($V_{\rm high}$, 40°–60°N, solid line) and that in the low latitudes ($V_{\rm low}$, 15°–30°N, dashed line). (b) $\Delta V = V_{\rm high} - V_{\rm low}$ (solid line), as an index for the zonally averaged meridional divergence ($\Delta V > 0$: divergence; $\Delta V < 0$: convergence) in the middle latitudes. Thick and thin grey lines are the cycle-length (CL) and the intensity of the 11-yr solar cycle, respectively, based on Fig. 1.

activity even on the interdecadal timescales. Such difference of the meridional circulations between the low and high solar activities must result in very different extreme weather/climate events regarding their pre-

ferred location and severity.

5. Solar activity and the ENSO cycle

The ENSO is a coupled ocean-atmospheric phenomenon on the interannual timescales with the averaged timescale of 4 yrs having a QBO component (e.g., Trenberth, 1997). The solar activity discussed in this work is on the decadal timescale and longer. Thus, there is no one-to-one relationship between a phase of the 11-yr solar cycle and a phase of the ENSO cycle. However, the composites of the skin temperature in the tropical Pacific show that the winters for SCmin (SCmax) in Figs. 6b (Fig. 6c) are likely related to El Niño (La Niña) events. This result is consistent with some earlier analyses (e.g., van Loon et al., 2007). It is interesting to search for a clue whether the contrast shown in the composite skin temperature patterns is simply a coincidence or there is some physical/dynamical mechanism for such a preferred phase relationship.

Beside the possible mechanism in the relationship between low/high solar activity and El Niño/La Niña events proposed in the previous studies, here we propose another possible mechanism. Even though the two phenomena are on different timescales, their relationship may be understood by the general circulation patterns favored by SCmin/SCmax presented in section 4. A possible link between solar activity and the phase of ENSO cycle was proposed as the following. SCmin (SCmax) favors stronger (weaker) and/or expanded (shrunk) Siberian high, which leads stronger (weakened) EAWM. Then, based on Li (1990), stronger EAWM might excite El Niño events by weakening the trade wind in the equatorial central to western Pacific area. Thus, an extremely low or high solar activity may enhance a favored, or weaken an unfavored, phase of the ENSO cycle. Since the ENSO cycle on the interannual timescales is mainly due to the nonlinear ocean-atmosphere system responding to the external annual forcing, and since the annual cycle is modulated by solar activity, some kind of phase relationship, though may not be stationary, could exist, which needs to be further explored.

In the following, we will use two cases to show that a phase of the ENSO cycle may not fundamentally change the basic features of the surface temperature and the circulation patterns in the high latitudes preferred by low or high solar activity shown in section 4.

As noticed in the Introduction, the 2009/2010 winter was highly unusual in many regions in Northern Hemisphere. Extremely cold and snowy weather events frequently occurred in northern and eastern China, Korea, eastern United States, and Europe, while much of Canada especially its eastern part, southwestern China, as well as the Arctic and the central tropical Pacific were unusually warm.[g] [h] [i] This winter not only had extremely larger anomalies in temperature and precipitation breaking many records in decades or even in modern history, but also had unusually longer duration than the normal meteorological winter season defined as December, January and February. Such extreme weather conditions in some regions are so persistent that started in November 2009 or earlier and extended into March 2010.[j] [k] The anomalous weather/climate events were also observed in the following summer and again in the winter of 2010/2011. In January 2011, the Arctic sea ice extent was the lowest on record, and the average temperature in China was the second lowest since national records began in 1961 behind 1977.[l] Although the two successive winters seem to be a couple of years after the latest SCmin, it is interesting to observe an El Niño event in the tropical Pacific in the 2009/2010 winter[m], while a La Niña event in the following 2010/2011 winter.

Figure 13 presents the comparison of the skin temperature, SLP, 850-hPa wind and the 500-hPa circulation characteristics between the 2009/2010 and 2010/2011 winters. The circulation features in the opposite phases of the ENSO cycle between the two winters exhibit the dominance of the QBO component in the ENSO cycle. Although there are opposite SST anomalies in the tropical Pacific between the two winters, the high-latitude skin temperature, especially the large-scale cold anomaly in the Siberian area, and the 500-hPa circulation patterns in both winters are largely similar to the SCmin features discussed in section 4.

The winters of 1988/1989 (La Niña) and 1991/1992 (El Niño) are selected as a pair of opposite phases of the ENSO cycle for SCmax (Fig. 14), when it is also

[g] http://www.ncdc.noaa.gov/sotc/?report=hazards&year=2009&month=12.
[h] http://www.ncdc.noaa.gov/sotc/?report=hazards&year=2010&month=1.
[i] http://www.ncdc.noaa.gov/sotc/?report=hazards&year=2010&month=2
[j] http://www.ncdc.noaa.gov/sotc/?report=hazards&year=2009&month=11.
[k] http://www.ncdc.noaa.gov/sotc/?report=hazards&year=2010&month=3
[l] http://www.ncdc.noaa.gov/sotc/global/2011/1
[m] It was actually an El Niño Modoki winter, not a canonical El Niño winter. It needs a further study to see whether and how solar activity may have impacted the preference of the ocean-atmospheric coupling system in the tropical Pacific to choose a canonical El Niño or an El Niño Modoki to occur. This subject is out of scope of this study.

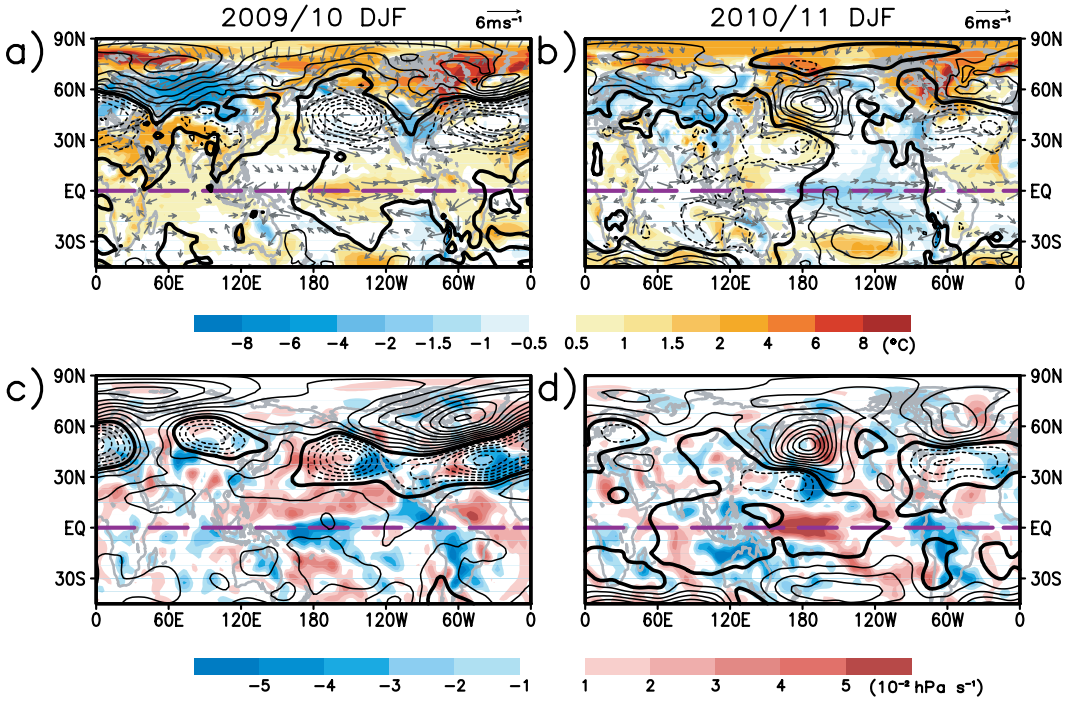

Fig. 13. Skin temperature (shaded), SLP (contours; interval: 2 hPa), and 850-hPa wind anomalies for (a) 2009/2010 DJF and (b) 2010/2011 DJF. 500-hPa vertical pressure velocity (shaded) and geopotential height anomalies (contours; interval: 20 m) for (c) 2009/2010 DJF and (d) 2010/2011 DJF. The wind vectors in (a) and (b) with magnitudes less than 0.5 m s^{-1} are neglected.

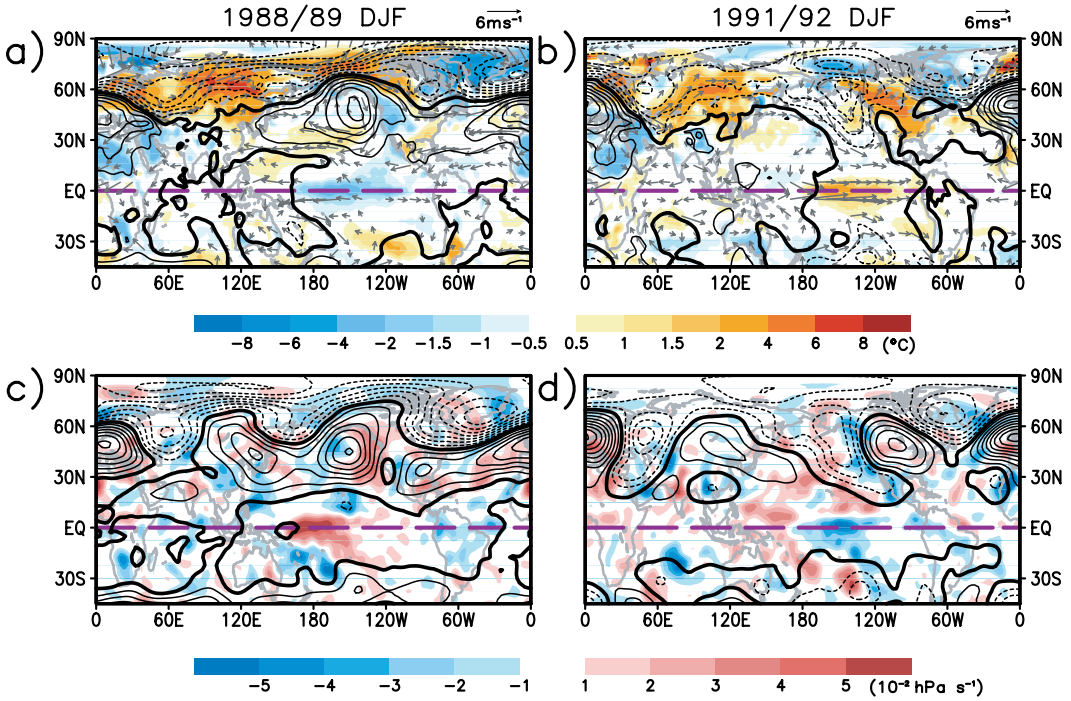

Fig. 14. Same as Fig, 13, except for the 1988/1989 and 1991/1992 winters.

in high solar activity on the interdecadal timescales (Fig. 12). Figure 14 is the counter part of Fig. 13. Despite the opposite phase of the ENSO cycle between the two winters, the high-latitude circulation patterns

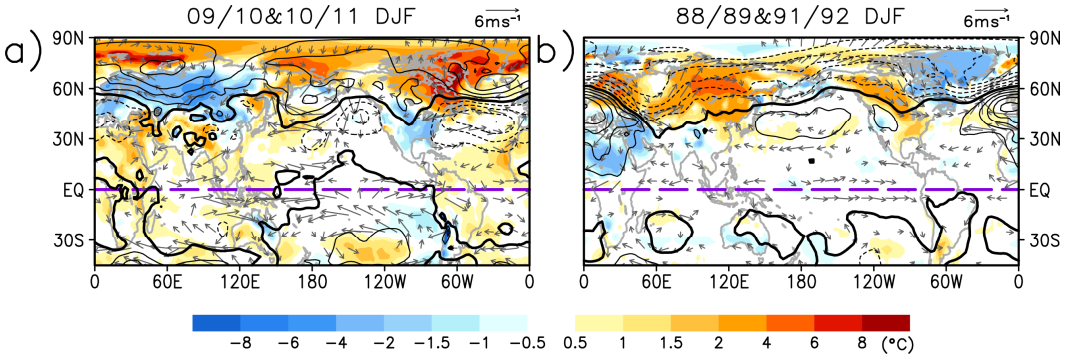

Fig. 15. The means of skin temperature (shaded), SLP (contours; interval: 2 hPa), and 850-hPa wind anomalies for (a) the 2009/2010 and 2010/2011 winters, and (b) the 1988/1989 and 1991/1992 winters.. The wind vectors in (a) and (b) with magnitudes less than 1 m s^{-1} are neglected.

in the two winters are largely similar, especially the large-scale positive skin temperature anomalies over the Siberian area, which is a main feature for SCmax. Note that, the pair of winters in Fig. 13 shows the dominance of the QBO component in the ENSO cycle, while the pair of winters in Fig. 14 shows a longer timescale of the ENSO cycle, which takes about 3 years from the peak La Niña winter of 1988/1989 to the peak El Niño winter of 1991/1992. In the latter ENSO cycle, the QBO component is very weak. To show the point that the high-latitude circulations are largely influenced by solar activity, not the ENSO events, we present some averaged fields for each of the pair in Fig. 15.

Figure 15a presents the mean fields of the two winters of 2009/2010 and 2010/2011 in Figs. 13a and 13b. As the result, the QBO component of the ENSO is largely removed, leaving a very weak positive skin temperature anomaly and convergent wind in the central tropical Pacific. The mean high-latitude land temperature, however, especially that over the Siberian area remains large-scale cold anomaly, which is associated with enhanced EAWM in the northeastern Asia. The mean NAM index for the two winters is kept negative (Fig. 11). The zonally averaged surface wind in the mid-latitude is convergent (also see Fig. 12), implying that more wave activity and more extreme climate events may happen there. The features in the middle and high latitudes are consistent with SCmin condition, in spite of the fact that the skin temperature in the tropical Pacific is largely opposite between the two winters.

Figure 15b is the mean fields for the two winters of 1988/1989 and 1991/1992 shown in Figs. 14a and 14b. The averaging has largely removed the ENSO signal, leaving a very weak negative skin temperature anomaly and divergent wind in the central tropical Pacific. In the middle and high latitudes, the mean skin temperature, especially the large-scale warm anomaly in the Siberian area, and the atmospheric circulations largely exhibit similar features to those for SCmax discussed in section 4. The EAWM in the northeastern Asia is weakened, which is mainly due to weakened Siberian high. The zonally averaged surface wind in the mid-latitude is divergent (also see Fig. 12). The mean NAM index for the two winters is positive (Fig. 11).

The opposite large-scale mean skin temperature anomalies in the Siberian area and associated very different SLP and mid-latitude circulation patterns between the two pairs of winters (Fig. 15) reflect the solar influence on the surface temperature and atmospheric circulations, as well as the location and severity of extreme weather/climate events, on the interdecadal timescales regardless of the phase of the ENSO cycle. Therefore, although a possible solar influence on a preferred ENSO phase was suggested in this section, a solid phase relationship between the solar activity on the decadal-interdecadal timescale and the ENSO cycle on the interannual timescale has not been established based on the limited data analysis provided here. As will be presented in Part II, the phase between the 11-yr solar activity and the ENSO cycle may be time-dependent due to the modulation by long-term solar activity, which is much more complicated than the examples presented here.

6. Summary and concluding remarks

Part I of this study presents a "bottom up" mechanism that amplifies the impacts of solar activity on the surface temperature and atmospheric circulations on the decadal-interdecadal timescales in the Northern Hemisphere winter. The solar modulation of annual cycle changes the thermal contrast at the earth surface between latitudes and that between land and ocean, which in turn change the atmospheric wave in-

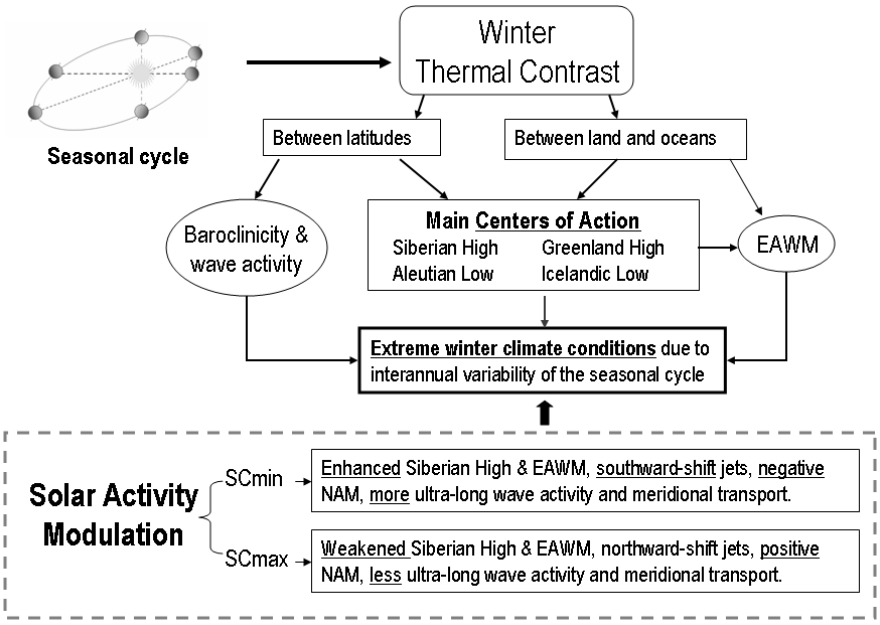

Fig. 16. Summary of the "bottom-up" amplifying mechanism for the solar impacts on winter climate in the Northern Hemisphere.

stability and circulation patterns, including EAWM, in different ways between low and high solar activity on multiple timescales. Thus, the atmospheric dynamics plays an important role to amplify the solar impacts on the general circulation patterns that are closely related to extreme weather/climate events. This "bottom-up" amplifying mechanism is summarized and sketched in Fig. 16.

Here are concluding remarks for Part I:

- The atmospheric dynamical processes amplify the solar thermal impacts on climate even when the change in the TSI over multi-scale solar activity is small. For SCmin (SCmax), in the Northern Hemisphere winter, the enhanced (reduced) meridional temperature gradient enhances (weakens) ultra-long baroclinic wave activity. The enhanced (reduced) land-ocean thermal contrast enhances (weakens) topographic waves. The amplified (weakened) mid-latitude waves transport more (less) heat from the low- to high-latitudes, so that the efficiency of the atmospheric "heat engine" is enhanced (reduced) for SCmin (SCmax). Different atmospheric circulation patterns between low and high solar activity cause extreme weather/climate events to occur in different locations with different severity. It should be kept in mind that once a solar preferred atmospheric circulation patterns and related weather/climate events occur, the nonlinear wave-mean interaction will be in effect, resulting in zonal index cycle, which may or may not synchronize with solar activity. Therefore, the circulation patterns on synoptic timescales are more complex than the ones presented here for winter climate conditions influenced by the multi-scale solar activity.

- The fundamental mechanism for solar impacts on climate must be "bottom-up". The bottom-up mechanism is able to explain how a change in the TSI can directly change the thermal contrasts on the earth surface, which is the driving force of the atmospheric circulations. The latter is closely related to extreme weather/climate events and climate change, which occur in the lower troposphere near the surface, where the human is living and more concern with its climate condition. The "top-down" mechanisms cited in the Introduction, though useful, can only play indirect roles in solar impacts on climate.

- On decadal-interdecadal timescales, solar activity exerts more influence on the atmospheric circulations in the high latitudes than those in the low latitudes, where the ENSO/QBO influences on climate are dominant. In the mid-latitudes, both influences are in effect and interact. Whether the polar region is warm or cold than normal is determined by the heat balance between the direct warming due to more solar incoming energy and the indirect cooling due to less poleward heat transport for high solar activity, or between the direct cooling due to less

solar incoming energy and the indirect warming due to more poleward heat transport for low solar activity.

- In order to properly estimate the anthropogenic impacts on climate, we must first understand and properly estimate the impacts of solar activity on climate. Since the anthropogenic and volcanic forcing scenarios in climate models, though not studied in this work, do not influence the climate in the same way as the sun does, i.e., those forcings do not involve in the dynamical amplifying mechanism as the solar activity does, the attribution studies that use simple comparison of the thermal impacts among different external forcings on the global and regional temperature would underestimate the solar impacts on climate. Without properly estimating the solar impacts, an estimation of anthropogenic impacts on climate would not be justified. Such results may not provide useful information for the policy makers to make right decisions regarding the preparation for, and mitigation of, possible climate disasters and the proper use of favorite climate conditions during climate change.

- The causes of modern climate change and climate extremes have been a controversial issue over the past several decades. As a contribution to this debate, the current study provides a "bottom-up" atmospheric amplifying mechanism of solar impacts on climate extremes presented here has not yet been well understood and simulated by numerical climate models. More studies from the viewpoint of atmospheric dynamics are needed to further explore the solar impacts on climate variability and related extreme climate events.

In order to understand and estimate how often the solar impacted climate extremes may reoccur, i.e., to find the dominant timescales of their occurrence and the multi-scale earth surface warming over the 20th century, we must also understand some basic principles of the nonlinear sun-climate forcing-response relationship in the time domain, which will be studied in Part II (Weng, 2012).

Acknowledgements. The author was a visiting scientist at the LASG of the Institute of Atmospheric Physics, Chinese Academy of Sciences. Her special thanks go to Profs. WU Guoxiong, WANG Bin and LU Riyu at LASG for their kind supports and encouragements. She is thankful to many colleagues at LASG for their various helps during her visit. Her deep appreciation goes to Zuojun YU for her various helpful discussions, and to Kaidi WENG for his long-term technical support and encouragement for the author to complete this sun-climate research. She also thanks Dr. Willie SOON and an anonymous reviewer for their many constructive comments to improve the final two-part manuscripts. She greatly appreciates the generous financial support provided by the LASG State Key Laboratory Special Fund for this research project.

REFERENCES

Barry, L., G. C. Craig, and J. Thuburn, 2002: Poleward heat transport by the atmospheric heat engine. *Nature*, **415**, 774–777.

Brohan, P., J. J. Kennedy, I. Harris, S. F. B. Tett, and P. D. Jones, 2006: Uncertainty estimates in regional and global observed temperature changes: A new data set from 1850. *J. Geophys. Res.*, **111**, D12106, doi: 10.1029/2005JD006548.

Camp, C. D., and K.-K. Tung, 2007: Surface warming by the solar cycle as revealed by the composite mean difference projection. *Geophys. Res. Lett.*, **34**, L14703, doi: 10.1029/2007GL030207.

Ding, Y., and T. Krishnamurti, 1987: Heat budget of the Siberian High and the winter monsoon. *Mon. Wea. Rev.*, **115**, 2428–2449.

Gleissberg, W., 1965: The eighty-year solar cycle in auroral frequency numbers. *Journal of the British Astronomical Association,* **75**, 227.

Gong, D.-Y., and C.-H. Ho, 2002: The Siberian high and climate change over middle to high latitude Asia. *Theor. Appl. Climatol.*, **72**, 1–9.

Gray, L. J., and Coauthors, 2010: Solar influences on climate. *Rev. Geophys.*, **48**, RG4001.

Haigh, J. D., 2007: The Sun and the Earth's climate. *Living Rev. Solar Phys.*, **4**, lrsp-2007-2. [Available online from http://www.livingreviews.org/lrsp-2007-2]

Ineson, S., A. A. Scaife, J. R. Knight, J. C. Manners, N. J. Dunstone, L. J. Gray, and J. D. Haigh, 2011: Solar forcing of winter climate variability in the Northern Hemisphere. *Nature Geoscience,* doi: 10.1038/NGEO1282.

IPCC, 2007: *Climate Change 2007: The Physical Science Basis. Contribution of Working Group I to the Fourth Assessment Report of the Intergovernmental Panel on Climate Change*, Solomon et al., Eds., Cambridge University Press, Cambridge and New York, 996pp.

Jin, F.-F., J. D. Neelin, and M. Ghil, 1996: El Niño/Southern Oscillation and the annual cycle: Subharmonic frequency-locking and aperiodicity. *Physics D*, **98**, 442–465.

Kalnay, E., and Coauthors, 1996: The NCEP/NCAR 40-year reanalysis project. *Bull. Amer. Meteor. Soc.,* **77**, 437–471.

Kerr, R. A., 2000: A North Atlantic climate pacemaker for the centuries. *Science*, **288**(5473), 1984–1986.

Kodera, K., and Y. Kuroda, 2005: A possible mechanism of solar modulation of the spatial structure of the North Atlantic Oscillation. *J. Geophys. Res.*, **110**,

D02111, doi: 10.1029/2004JD005258.

Labitzke, K., and H. van Loon, 1988: Association between the 11-year solar cycle, the QBO, and the atmosphere, I, The troposphere and stratosphere on the Northern Hemisphere winter. *J. Atmos. Terr. Phys.*, **50**, 197–206.

Lean, J., 1991: Variations in the sun's radiative output. *Rev Geophys,* **29**, 505–535.

Lean, J. L., and D. H. Rind, 2009: How will Earth's surface temperature change in future decades? *Geophys. Res. Lett.*, **36**, L15708, doi: 10.1029/2009GL038932.

Li, C., 1990: Interaction between anomalous winter monsoon in East Asia and El Niño events. *Adv. Atmos. Sci.*, **7**, 36–46.

Li, J., and J. Wang, 2003: A modified zonal index and its physical sense. *Geophys. Res. Lett.,* **30**, 1632, doi: 10.1029/2003GL017441.

Lindzen, R. S., 1994: Climate dynamics and global change. *Annual Review of Fluid Mechanics*, **26**, 353–378.

Lorenz, E. N., 1967: *The Nature and Theory of the General Circulation of the Atmosphere.* WMO, Geneva, 161pp.

Matsuno, T., 1971: A dynamical model of the stratospheric sudden warming. *J. Atmos. Sci.*, **28**, 1479–1494.

Meehl, G. A., J. M. Arblaster, G. Branstator, and H. van Loon, 2008: A coupled air-sea response mechanism to solar forcing in the Pacific region. *J. Climate*, **21**, 2883–2897, doi: 10.1175/2007JCLI1776.1.

Nakamura, H., T. Izumi, and T. Sampe, 2002: Interannual and decadal modulations recently observed in the Pacific storm track activity and East Asian winter monsoon. *J. Climate*, **15**, 1855–1874.

NRC, 1994: *Solar Influences on Global Change.* Natl. Acad., Washington, D.C., USA, 163pp.

Rayner, N. A., D. E. Parker, E. B. Horton, C. K. Folland, L. V. Alexander, D. P. Rowell, E. C. Kent, and A. Kaplan, 2003: Global analyses of SST, sea ice and night marine air temperature since the late nineteenth century. *J. Geophys. Res.*, **108**, doi: 10.1029/2002JD002670.

Reid, G. C., 1991: Solar total irradiance variations and the global sea surface temperature record. *J. Geophys. Res.*, **96**, 2835–2844.

Robock, A., 2002: The climatic aftermath. *Science*, **295**, 1242–1244.

Roy, I., and J. D. Haigh, 2010: Solar cycle signals in sea level pressure and sea surface temperature. *Atmos. Chem. Phys.*, **100**, 3147–3153.

Salby, M., and P. Callaghan, 2004: Evidence of the solar cycle in the general circulation of the stratosphere. *J. Climate*, **17**, 34–46.

Shindell, D., D. Rind, N. Balachandran, J. Lean, and P. Lonergran, 1999: Solar cycle variability, ozone, and climate. *Science*, **284**, 305–308.

Semenov, V. A., M. Latif, D. Dommenget, N. S. Keenlyside, A. Strehz, T. Martin, and W. Park, 2010: The Impact of North Atlantic–Arctic multidecadal variability on Northern Hemisphere surface air temperature. *J. Climate,* **23**, 5668–5677.

Soon, W., 2009: Solar arctic-mediated climate variation on multidecadal to centennial timescales: Empirical evidence, mechanistic explanation, and testable consequences. *Physical Geography*, **30**, 144–184.

Soon, W., K. Dutta, D. R. Legates, V. Velasco, and W.-J. Zhang, 2011: Variation in surface air temperature of China during the 20th century. *Journal of Atmospheric and S olar-Terrestrial Physics*, **73**, 2331–2344.

Trenberth, K. E., 1997: The definition of El Niño. *Bull. Amer. Meteor. Soc.*, **78**, 2771–2777.

Tung, K.-K., and R. S. Lindzen, 1979: A theory of stationary waves. Part I: A simple theory of blocking. *Mon. Wea. Rev.*, **107**, 714–734.

Tung, K.-K., and D. C. Camp, 2008: Solar-cycle warming at the earth's surface in NCEP and ERA40 data: A linear discriminant analysis**.** *J. Geophys. Res.,* **113**, DO5114, doi: 10.1029/2007JD009164.

van Loon, H., G. A. Meehl, and J. S. Dennis, 2007: Coupled air-sea response to solar forcing in the Pacific region during northern winter. *J. Geophys. Res.*, **112**, D02108, doi: 10.1029/2006JD007378.

Wallace, J. M., and D. W. J. Thompson, 2002: The Pacific center of action of the Northern Hemisphere annular mode: Real or artifact? *J. Climate*, **15**, 1987–1991.

Weng, H.-Y., 2005: The influence of the 11 yr solar cycle on the interannual-centennial climate variability. *Journal of Atmospheric and Solar-Terrestrial Physics*, **67**, 793–805.

Weng, H.-Y., 2012: Impacts of multi-scale solar activity on climate. Part II: Dominant timescales in decadal-centennial climate variability. *Adv. Atmos. Sci.*, **29**(4), 887–908, doi: 10.1007/s00376-012-1239-0.

Weng, H.-Y., and A. Barcilon, 1988: Wavenumber selection for single-wave steady states in a nonlinear baroclinic system. *J. Atmos. Sci.*, **45**, 1039–1051.

Weng, H.-Y., and K.-M. Lau, 1994: Wavelets, period doubling, and time-frequency localization with application to organization of convection over the tropical western Pacific. *J. Atmos. Sci.*, **51**, 2523–2541.

White, W. B., J. Lean, D. R. Cayan, and M. D. Dettinger, 1997: Response of global upper ocean temperature to changing solar irradiance. *J. Geophys. Res.*, **102**, 3255–3266.

Zhou, T., and R. Yu, 2006: Twentieth-century surface air temperature over China and the globe simulated by coupled climate models. *J. Climate*, **19**, 5843–5858.